

Angular distributions of scattered excited muonic hydrogen atoms*

V.N. Pomerantsev, V.P. Popov
Institute of Nuclear Physics, Moscow State University

Differential cross sections of the Coulomb deexcitation in the collisions of excited muonic hydrogen with the hydrogen atom have been studied for the first time. In the framework of the fully quantum-mechanical close-coupling approach both the differential cross sections for the $nl \rightarrow n'l'$ transitions and l -averaged differential cross sections have been calculated for exotic atom in the initial states with the principle quantum number $n = 2 - 6$ at relative motion energies $E_{\text{cm}} = 0.01 - 15$ eV and at scattering angles $\theta_{\text{cm}} = 0 - 180^\circ$. The vacuum polarization shifts of the ns -states are taken into account. The calculated in the same approach differential cross sections of the elastic and Stark scattering are also presented. The main features of the calculated differential cross sections are discussed and a strong anisotropy of cross sections for the Coulomb deexcitation is predicted.

Introduction. Exotic hydrogen-like atoms are formed in excited states, when heavy negative particles (μ^- , π^- , etc.) are slowed down and captured in hydrogen media. The following atomic cascade of collisional and radiative transitions proceeds via many intermediate states up to nuclear absorption or transition to the ground state occurs. Since the experimental data are mainly available for the last stage of this atomic cascade, the reliable knowledge of the total and differential cross sections (DCS) of the collisional processes during the cascade is needed for the realistic analysis of these data.

In particular, the collisional processes

$$(\mu^- p)_{nl} + H_{1s} \rightarrow (\mu^- p)_{n'l'} + H_{1s} \quad (1)$$

of the elastic scattering ($n' = n$, $l' = l$), Stark transitions ($n' = n$, $l' \neq l$), and Coulomb deexcitation ($n' < n$) essentially change the energy- and nl -distributions of exotic atoms. It is especially important from the view of the precise experiments at the Paul Scherrer Institute with muonic [1] and pionic [2] hydrogen atoms. These experiments are aimed at the extraction of the root mean squared proton charge radius with the relative accuracy of 10^{-3} from the Lamb shift experiment [1] and the determination of the πN scattering lengths with the accuracy better than 1% by extracting the shift and width of $1s$ state due to the strong interaction in pionic hydrogen [2]. The proper analysis of these experiments requires a reliable theoretical treatment of related cascade processes.

The Coulomb deexcitation (CD) plays an important role in the kinetic energy distribution of the exotic atoms. In particular, the energy distribution of $(\mu^- p)$ - and $(\pi^- p)$ - atoms during the radiative transitions $np \rightarrow 1s$ have significant high-energy components resulting from the preceding Coulomb deexcitation transitions. Before the recent paper [3] the only $\Delta n = 1$ transitions are assumed to be important in the Coulomb transitions at low n . Moreover, it is also suggested in the cascade calculations [4] that the CD process results in the isotropic angular distribution.

The main goal of this paper is to introduce the first theoretical study of the Coulomb deexcitation differen-

tial cross sections in the muonic atom – hydrogen atom collisions. In particular, we are interested in the main features of the n and E dependences of these cross sections. Our new results, concerning the DCS of elastic and Stark scattering are also presented.

The first theoretical study of DCS for the elastic and Stark scattering in the collisions of the excited exotic atom from atomic hydrogen has been performed within the quantum-mechanical adiabatic approach [5]. Later, these cross sections were also calculated in the framework of the close-coupling model and semiclassical approximation [6] where the Coulomb interaction of the exotic atom with the hydrogen atom field is modeled by the screening dipole approximation. This approximation becomes invalid at low collisional energies below some value E^* , which depends on the principal quantum number n (see [7]). Thus, the latter approach as well as various modifications of the semiclassical model [8, 9] can result in uncontrolled errors in the low-energy region where only a few partial waves are important.

In the present paper the DCS of the processes (1) are studied in the framework of the more accurate close coupling (CC) approach. The approach has been developed earlier [10] by the authors to describe the elastic scattering and Stark transitions in the exotic atom – hydrogen molecule collisions and employed recently [3] to give a unified treatment of the processes (1). In the framework of the CC approach the first fully quantum-mechanical calculations of the total cross sections of the Coulomb deexcitation both for muonic [3] and pionic [11] hydrogen atoms have been performed.

Approach. In the framework of the close-coupling approach the total wave function of the four-body system is expanded in terms of the basis states with the conserving quantum numbers of the total angular momentum JM and parity $\pi = (-1)^{l+L}$. The basis states are chosen as tensor products of the corresponding wave functions of the free exotic and hydrogen atoms and the angular wave function of their relative motion. This expansion results in the set of the coupled differential equations. In contrast with paper [6], in the present approach the interaction potential matrix for the exact four-body Coulomb interaction of the colliding atoms is calculated analytically. Moreover, as it is shown in paper [3] the approximation similar to "dipole approximation" results in an improper description of the CD process, especially

*This work was partially supported by Russian Foundation for Basic Research, grant No. 03-02-16616.

for the low-lying states of the exotic atom.

At fixed E_{cm} (energy of collision in the center of mass system) and given J and π the set of the coupled equations are solved numerically by the Numerov method with the standing-wave boundary conditions involving the real and symmetrical K -matrix. The corresponding T -matrix can be obtained from the K matrix using the matrix equation $T = 2iK(I - iK)^{-1}$. In the present study, as distinct from paper [3], we take into account the energy shifts of the ns states due to the vacuum polarization which are very important especially at the low kinetic energies comparable with the energy shift and for the lower states of the exotic atom. The $2s - 2p$ energy splitting $\Delta\varepsilon_{2s-2p}$ for the muonic hydrogen atom is equal to 0.206 eV and this splitting decreases approximately as n^{-3} with n increasing.

The formalism has been described in more details in [3]. Here we give only the formulas for the DCS. The differential cross sections for the transition from the initial state (nl) to the final state ($n'l'$) are defined as

$$\frac{d\sigma_{nl \rightarrow n'l'}}{d\Omega} = \frac{1}{2l+1} \frac{k_f}{k_i} \sum_{mm'} |f_{nlm \rightarrow n'l'm'}(k_i, k_f; \Omega)|^2, \quad (2)$$

where the scattering amplitude for the transition $nlm \rightarrow n'l'm'$ is given by

$$f_{nlm \rightarrow n'l'm'}(k_i, k_f; \Omega) = \frac{2\pi i}{\sqrt{k_i k_f}} \sum_{JLL'\lambda'} i^{L'-L} Y_{L0}^*(0) \langle lmL0 | Jm \rangle T_{nlL \rightarrow n'l'L'}^J \langle l'm'L'\lambda' | Jm \rangle Y_{L'\lambda'}(\Omega). \quad (3)$$

Here, k_i and k_f are the cms relative momenta in the initial and final channels, correspondingly; $\Omega \equiv \theta, \varphi$, where θ is the cms scattering angle, and $T_{i \rightarrow f}^J$ is the transition matrix in the total angular momentum representation. The indices of the entrance channel and the target electron state are omitted for brevity.

In order to illustrate the most general features of DCS, it is also useful to introduce the cross sections averaged over the initial orbital angular momentum l of the exotic atom. So, the following l -averaged angular distributions are also discussed in the present study: for elastic scattering

$$\frac{d\sigma_n^{el}}{d\Omega} = \frac{1}{n^2} \sum_l (2l+1) \frac{d\sigma_{nl \rightarrow nl}}{d\Omega}, \quad (4)$$

for Stark transitions

$$\frac{d\sigma_n^{St}}{d\Omega} = \frac{1}{n^2} \sum_{l,l'} (1 - \delta_{ll'}) (2l+1) \frac{d\sigma_{nl \rightarrow n'l'}}{d\Omega}, \quad (5)$$

and, finally, for CD process

$$\frac{d\sigma_{n \rightarrow n'}^{CD}}{d\Omega} = \frac{1}{n^2} \sum_{l,l'} (2l+1) \frac{d\sigma_{nl \rightarrow n'l'}}{d\Omega}, \quad n' < n. \quad (6)$$

Hereafter, the atomic units will be used throughout the paper and the collision energy will be referred to the

states with $l \neq 0$ in the entrance channel, which are assumed to be degenerated.

Results. The numerical calculations of the DCS for the collisional processes (1) have been done for $(\mu p)_n$ atoms with the initial principal quantum number values $n = 2 - 6$ at the relative motion energies $E_{cm} = 0.01 - 15$ eV and at all the scattering angles θ_{cm} from zero up to 180° . All the exotic-atom states corresponding to the open channels have been included in the close-coupling calculations. Some of our results are present here in Figs. 1 - 9 both for the cross sections of the separate $nl \rightarrow n'l'$ transitions and for the l -averaged ones.

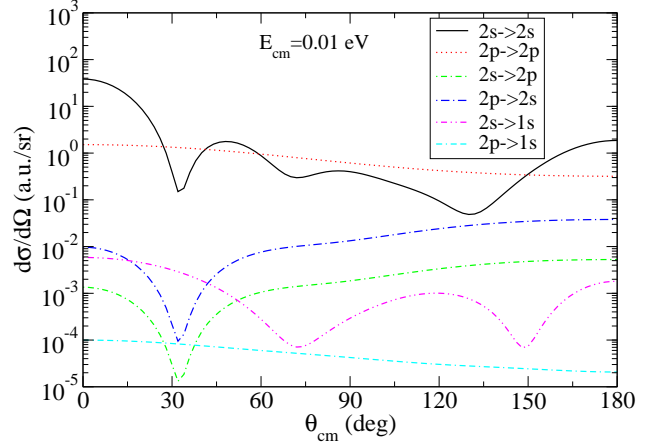


FIG. 1: Differential $2l \rightarrow 2l'$ and $2l \rightarrow 1s$ cross sections for $(\mu p)_{2l} + H$ collisions vs. cms scattering angle θ_{cm} at $E_{cm} = 0.01$ eV (referring to $2p$ state).

In Figs. 1 and 2 the DCS for $2p \rightarrow 2p, 2s$ (elastic and Stark scattering) and $2p \rightarrow 1s$ (Coulomb deexcitation) transitions versus cms scattering angle θ_{cm} at energies $E_{cm} = 0.01$ eV and 1 eV (referring to the $2p$ threshold) are shown. It is worthwhile noting that the relative motion energy in the entrance channel for the $2s \rightarrow 2s, 2p$ and $2s \rightarrow 1s$ transitions increases due to the Lamb shift $\Delta\varepsilon_{2s-2p} = 0.206$ eV in comparison with the scattering processes of the muonic hydrogen atom in the $2p$ state. As it is seen from Fig. 1, the angular distributions of the elastic $2p \rightarrow 2p$ scattering and Coulomb $2p \rightarrow 1s$ transition are similar and almost isotropic, their shapes are mainly defined by the contributions of the S -wave relative motion with a small mixture of the P -wave.

It is also seen that Coulomb deexcitation process for $2p \rightarrow 1s$ transition is more than four order of the magnitude suppressed relatively to the $2p \rightarrow 2p$ elastic scattering one and more or about two order of the magnitude as compared with both the Stark $2p \rightarrow 2s$ and Coulomb $2s \rightarrow 1s$ transitions, respectively.

The Stark transitions $2p \rightarrow 2s$ and $2s \rightarrow 2p$ are strongly inelastic at such a low energy (the initial and final energies differ more than twenty times) and that results in their quite unusual angular distributions (see Fig. 1) with the maximum at zero scattering angle and minimum at $\theta_{cm} \sim 30^\circ$ and smooth increasing at the backward hemisphere.

In the DCS of the elastic $2s \rightarrow 2s$ scattering ($E_{cm} =$

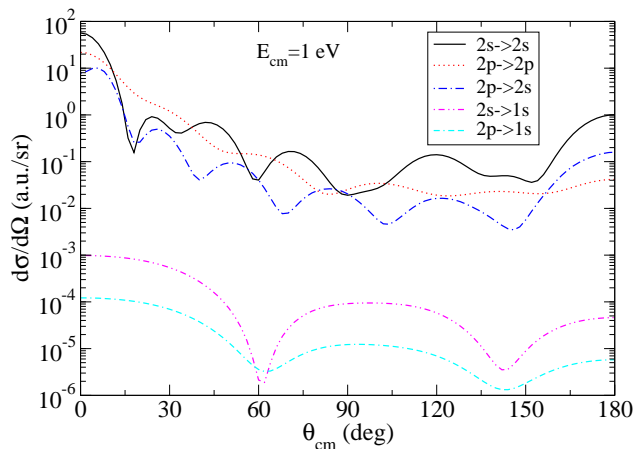


FIG. 2: The same as in Fig. 1 but at $E_{cm} = 1$ eV.

0.216 eV) we see the structures (due to higher partial waves, involved in the scattering process) as compared with the almost isotropic DCS for $2p \rightarrow 2p$ transition. The comparison of the DCS of the Stark transitions, presented in Figs. 1 and 2, shows a significant effect of the Lamb shift on these cross sections, which changes substantially depending on the ratio value of the $E_{cm}/\Delta\varepsilon_{2s-2p}$. The Stark DCS of the $2p \rightarrow 2s$ and $2s \rightarrow 2p$ transitions at low kinetic energy comparable with the Lamb shift value have quite different behavior in comparison with the elastic ones and reveal a strong suppression in the forward hemisphere by more than three order of the magnitude. When the energy of the collision is much larger than $\Delta\varepsilon_{2s-2p}$ we observe the usual picture [5, 6] of the DCS for Stark transitions with a strong forward peak and a set of maxima and minima (see Fig. 2).

Coulomb deexcitation process occurs at essentially smaller distances than the elastic and Stark processes. So, the number of partial waves involved in the CD process, as a rule, is much smaller, as a strong centrifugal barrier prevents the colliding atoms from penetrating in the interaction region corresponding to the process. With decreasing the value n the number of the partial waves contributing to the CD process (at the fixed energy) also decreases.

In particular, the DCS of the CD process in case of $n = 2$ have a quite simple angular dependence due to a few partial waves involved in the process (see Fig. 1 and 2). The angular dependences of the DCS for $2s \rightarrow 1s$ and $2p \rightarrow 1s$ Coulomb transitions are mainly determined by the contributions of the lowest partial waves of the relative motion at all energies under consideration. The differential cross sections of these Coulomb transitions as it is seen in Fig. 2 have a similar angular dependence which shape is slowly changed enhancing the forward hemisphere scattering with energy increasing.

It is well-known that in the muonic hydrogen atoms, the $2s$ -state plays a particular role due to $2s$ Lamb shift and has no analog in the other exotic atoms in which the strong interaction leads to a large rate of the nuclear absorption from this state. In particular, a new knowledge about the collisional quenching of $2s$ state at collisional energy near or below the $2p$ threshold is of special inter-

est.

As it shown in Fig. 1, the DCS for the $2p \rightarrow 1s$ transition is strongly suppressed in comparison with the main $2s \rightarrow 1s$ transition about two order of the magnitude and this suppression is also observed at higher kinetic energy (see also Fig. 2). Hence the $2s \rightarrow 1s$ transition determines the CD $2 \rightarrow 1$ transition at all kinetic energies and it is quite probable that the observed collisional quenching of the metastable $2s$ state of the muonic atom and the high energy component of muonic hydrogen in $1s$ state can be explained by the direct Coulomb deexcitation process.

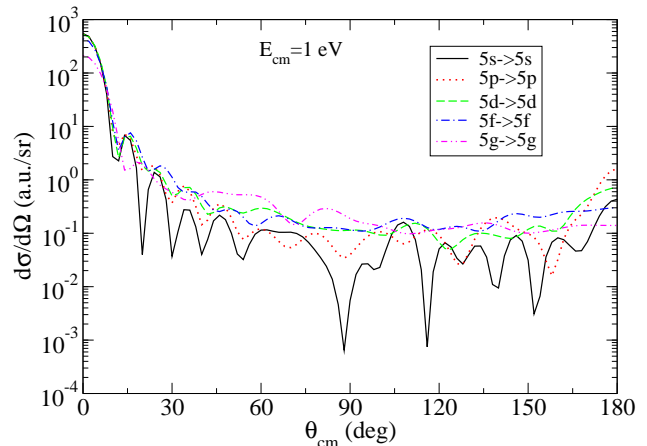


FIG. 3: Differential elastic ($l = l'$) cross sections for $(\mu p)_{5l} + H$ collisions vs. cms scattering angle θ_{cm} at $E_{cm} = 1$ eV.

The typical angular distributions for the individual $nl \rightarrow nl'$ transitions for $n = 5$ are shown in Fig. 3 and Fig. 4 for the elastic scattering and Stark transitions, respectively. It is well known [5, 6] that DCS of these processes are similar to the diffraction scattering (at the collisional energies more or about 1 eV) with a strong forward peak which is enhanced with increasing energy and a set of maxima and minima. While the elastic cross sections always have a strong peak at $\theta_{cm} = 0$, the first maximum position in the Stark DCS depends on the $\Delta l = |l - l'|$ value. In particular, for $\Delta l = 1$ this maximum is at finite scattering angles as it also remarked in [6]. According to our calculations, the sharpest variations in DCS are always observed in the $ns \rightarrow n's$ and $ns \rightarrow n'p$ transitions (see also Fig. 7 for DCS of the CD process).

The first and next peaks in the forward hemisphere for the elastic scattering (see Fig. 3) and Stark transitions (see Fig. 4) have a tendency to be less pronounced and the angular distribution becomes smoother with increasing l and Δl is increased. According to our calculations the shape of the peaks in the forward hemisphere is sharper with n increasing at the fixed collisional energy.

The dependence of the l -averaged DCS for the elastic scattering on the collisional energy is shown in Fig. 5 for $n = 4$. While the DCS for the individual elastic $nl \rightarrow nl$ transitions (the same is valid for the Stark $nl \rightarrow nl'$ transitions) reveal the complicated structure, the l -averaged cross sections smooth out many details and allow to study the most general features of the process. Figure 5 shows,

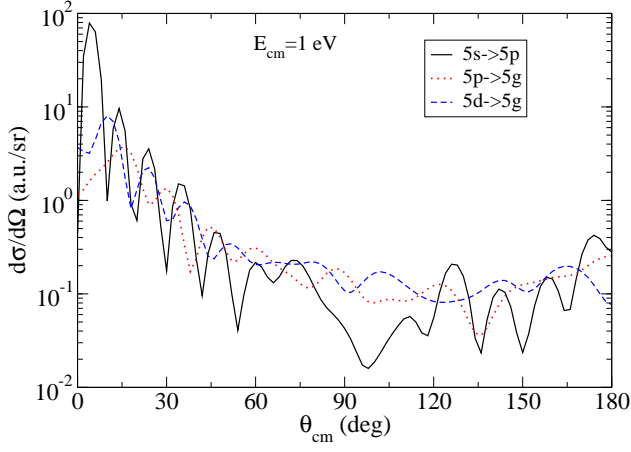


FIG. 4: Differential Stark cross sections for $5l \rightarrow 5l'$ transitions with $\Delta l = 1 - 3$ in $(\mu p) + H$ collisions at $E_{cm} = 1$ eV.

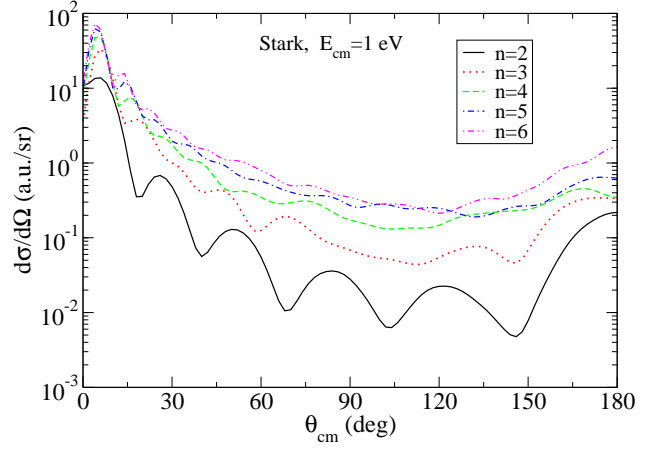


FIG. 6: The l -average differential Stark cross sections for $(\mu p)_n + H$ collisions ($n = 2 - 6$) at $E_{cm} = 1$ eV.

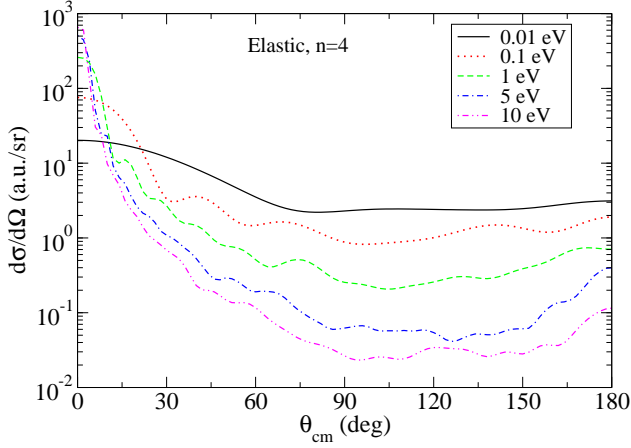


FIG. 5: The l -average differential elastic cross sections for $(\mu p)_{n=4} + H$ collisions at different energies.

that at low energies ($\lesssim 1$ eV) the DCS can be approximately considered as constant for the simple estimation at scattering angles θ_{cm} more or about 75° . However, at higher energies the appreciable enhancing of the backward scattering is observed.

In Fig. 6 we show the l -averaged Stark DCS at $E_{cm} = 1$ eV for different values of n . Here one can see that with the increase of n the first forward peak also becomes sharper and narrower (as well as for the elastic scattering) but remains to be at the finite values of scattering angle. The height of this peak depends on n not so strong as the diffraction maximum in elastic scattering (cf. Figs. 5 and 6). The diffraction structure of minima and maxima becomes less pronounced with increasing n . As a whole our results for the elastic and Stark DCS are in a qualitative agreement with the previous calculations [5, 6].

Now we are coming to the discussion of the typical angular distributions for the CD process. As far as we know, the calculations of these DCS have not been reported until now and in the cascade calculations the angular distributions of the CD process are presumed to be isotropic. The calculated DCS for individual $nl \rightarrow n'l'$ transitions with $\Delta n = 1$ and 2 at relative motion energy

$E_{cm} = 1$ eV are shown in Figs. 7 and 8, respectively. In Fig. 9 the l -averaged DCS for the $6 \rightarrow 5$ transition at different values of the relative motion energy from 0.01 up to 15 eV are presented.

Our study reveals the following main features of the CD angular distributions. The angular distributions both of the individual and l -averaged cross sections (excluding very low energies) are far from isotropic: as a whole the scattering at $\theta_{cm} \lesssim 60^\circ$ and $\theta_{cm} > 120^\circ$ is noticeably enhanced.

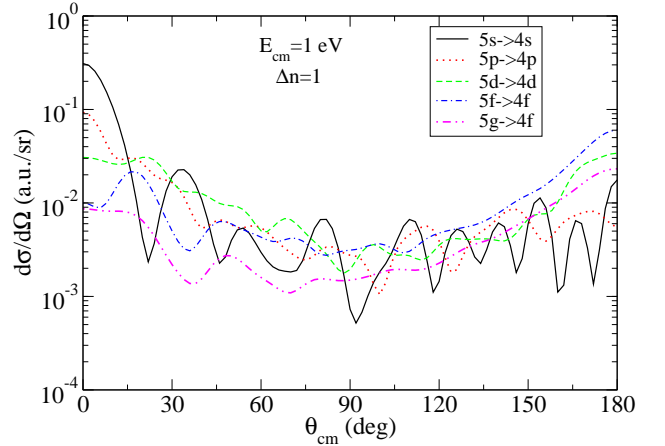


FIG. 7: Differential CD cross sections for the individual transitions with $\Delta n = 1$ for $n = 5$ at $E_{cm} = 1$ eV.

The DCS for $ns \rightarrow n's$ transitions (see Figs. 7, 8) have (as in case of the elastic scattering) a more pronounced diffraction structure with sharp maxima and minima and a strong peak at zero angle as compared with the smoother angular dependence for the other CD transitions. This behaviour can be simply explained by the conditions $L = L' = J$ (for $ns \rightarrow n's$ transitions) which strongly reduce the number of terms in the amplitude (3) in contrast with the other transitions.

The increase of kinetic energy enhances asymmetry in the angular dependence of the l -averaged DCS and decreases the role of the backward scattering (see Fig. 9).

Summary. The fully quantum-mechanical CC ap-

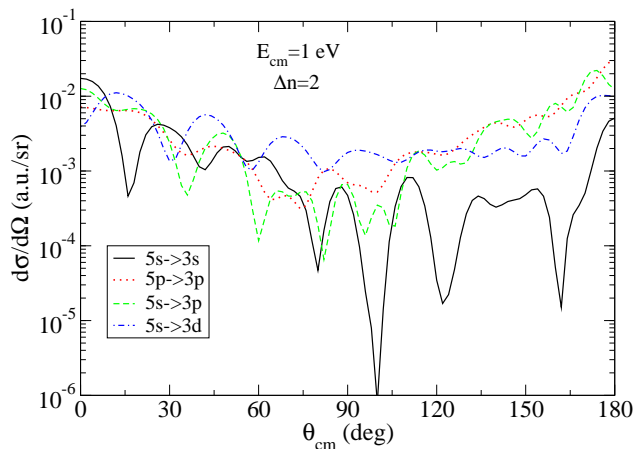


FIG. 8: The same as in Fig. 7 but for the $\Delta n = 2$ transitions.

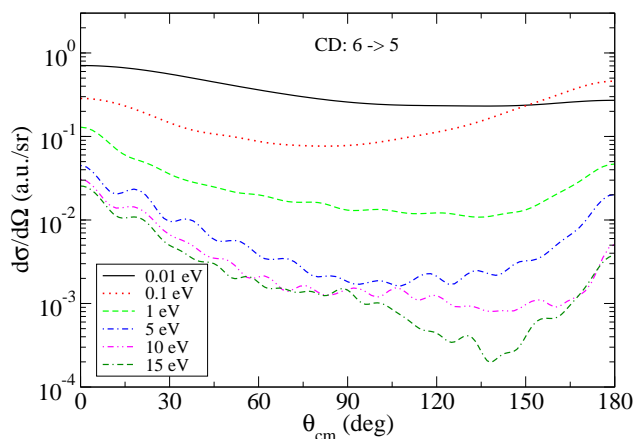


FIG. 9: The l -average CD differential cross sections for transition $6 \rightarrow 5$ at different energies.

proach has been applied for the calculations of the elastic scattering, Stark transition and Coulomb deexcitation DCS in a self-consistent manner and the detailed analysis of the obtained results has been performed. For the first time the DCS of the CD process have been calculated for the values of the principal quantum number and kinetic energy relevant for kinetics of the atomic cascade. The first results for the direct collisional quenching of the $2s$ -state due to CD process were also obtained. The present study reveals the new knowledge about the CD process and is very important for the reliable analysis of the K X-ray yields and high energy component in the kinetic energy distribution of muonic hydrogen atoms. We hope that our study allows to remove some uncertainties inherent in the previous cascade calculations, which resulted from the treatment of collisions, especially Coulomb deexcitation, involving different and not always self-consistent approximations.

We are grateful to Prof. G. Korenman for fruitful discussions.

-
- [1] F. Kottmann et al., *Hyperfine Interact.* **138**, 55 (2001).
 - [2] D. Gotta et al., *Newsletter* **15**, 276 (1999).
 - [3] G.Ya. Korenman, V.N. Pomerantsev, and V.P. Popov, *JETP Lett.* **81**, 543 (2005); nucl-th/0501036.
 - [4] T.S. Jensen and V.E. Markushin, physics/0205077.
 - [5] V.P. Popov and V.N. Pomerantsev, *Hyperfine Interact.* **119**, 137 (1999).
 - [6] T.S. Jensen and V.E. Markushin, PSI-PR-99-32(1999); physics/0205076; *Eur.Phys.Journ. D* **19**, 165 (2002).
 - [7] V.V. Gusev, V.P. Popov and V.N. Pomerantsev, *Hyperfine Interact.* **119**, 141 (1999).
 - [8] V. Bystritsky et al., *Phys. Rev. A* **53** (1996) 4169.
 - [9] T.P. Terada, R.S. Hayano, *Phys.Rev. C* **55**, 73 (1997).
 - [10] V.P. Popov and V.N. Pomerantsev, *Hyperfine Interact.* **138**, 109 (2001).
 - [11] V.N. Pomerantsev and V.P. Popov, nucl-th/0511026.